

Numerical investigation of stripe domain dynamics in grooved bubble garnet films

R. P. Morrissey,^{a)} M. Redjda, M. F. Ruane, and F. B. Humphrey
ECE Department, Boston University, 8 Saint Mary's Street, Boston, Massachusetts 02215

The dynamic behavior of an isolated stripe domain attracted to a single rectangular groove on the top surface of a 1.6- μm -thick bubble garnet film is analyzed using a numerical model based on the Landau–Lifshitz–Gilbert equation. The groove creates an effective field which interacts with the stripe domain, such that the azimuthal angle of magnetization in the wall no longer rotates uniformly through the film thickness. The wall shape becomes highly distorted near the groove, forming head-on walls at the groove corners, and cleaving when pushed beneath the groove. © 1999 American Institute of Physics. [S0021-8979(99)72608-3]

INTRODUCTION

Magnetic domain dimensions in magnetic computer memories have been steadily decreasing in order to support increased areal storage densities. As the storage density increases, however, it becomes increasingly important to confine the domains within a known area in order to avoid jitter associated with uncertainty in the location of a domain/bit. Topologically patterned materials have been investigated for some time as a possible means of pinning domain walls within a defined region.^{1,2} This technique has applications for magneto-optic, floptical, and vertical Bloch line (VBL) memory systems. In this article, we investigate the effects of a patterned single groove on the dynamic behavior of a stripe domain in its immediate vicinity.

TECHNIQUE

The investigation is performed by numerically solving the Landau–Lifshitz–Gilbert (LLG) equation on a Cartesian lattice with $160 \times 2 \times 240$ nodes, or 76 800 points. At each grid point, the solution to the LLG is computed using phenomenologically derived parameters for exchange, anisotropy, and saturation magnetization, in addition to an applied field. A fast three-dimensional (3D) Fourier transform based technique computes the demagnetizing field. This investigation concentrated on isolated (nonperiodic) two-dimensional (2D) problems by extending the magnetization distributions to infinity along one axis. A SGI Origin 2000 parallel supercomputer was used to perform the computations.

It is difficult to connect simulation results with corresponding effects in real materials. However, previous simulations performed using these techniques have obtained results consistent with observed behavior for these materials.³ These simulations consider infinite grooves with perfectly rectangular geometries, which do not perfectly model a real world situation with finite, imperfect grooves.

Initial magnetization distributions were obtained by inserting two otherwise identical walls of opposite chirality into the computational lattice and iteratively solving the LLG equation. An external field of -200 Oe was applied which

gave a stripe width of approximately $0.9 \mu\text{m}$. The walls, which bound the stripe domain, are parallel to each other and to the Y axis. The Z axis is perpendicular to the film surface, and the X axis is perpendicular to the wall plane.

Garnet material parameters are the exchange constant, $A = 3.0 \times 10^{-7}$ erg/cm; anisotropy field, $H_k = 1860$ Oe perpendicular to the film plane; saturation magnetization $4\pi M_s = 452$ G; and the gyromagnetic ratio $\gamma = 0.01$ Oe $^{-1}$ ns $^{-1}$. The simulations were performed with a Gilbert damping constant of $\alpha = 0.5$, but wall velocity calculations have been adjusted to reflect the true damping of $\alpha = 0.15$.

The film thickness was chosen to be $1.6 \mu\text{m}$ with a groove depth of 800 nm and a groove width of $1 \mu\text{m}$.

RESULTS AND DISCUSSION

A single stripe in bubble garnet film will have a width dependent upon the applied field and the domain demagnetizing field given by the material thickness and the saturation magnetization.⁴ The magnetization rotates uniformly from one domain orientation to the other through the thickness of the wall. A schematic cross section of a stripe domain is shown in Fig. 1.

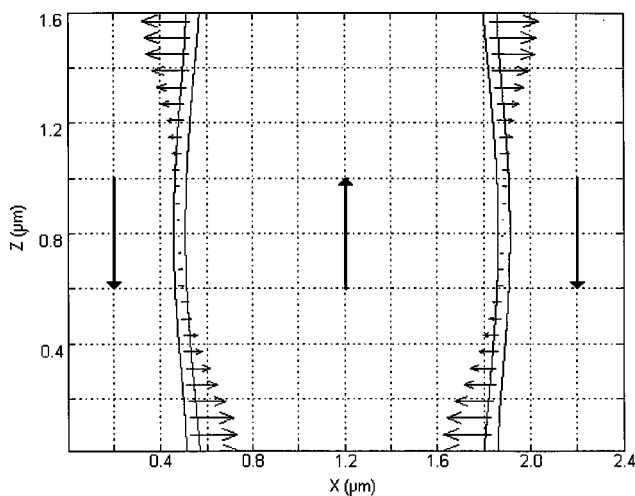


FIG. 1. Isolated stripe domain with walls indicated by 33%/66% contours showing in-plane magnetization angle ψ . The large arrows indicate the domain magnetization.

^{a)}Electronic mail: ronm@bu.edu

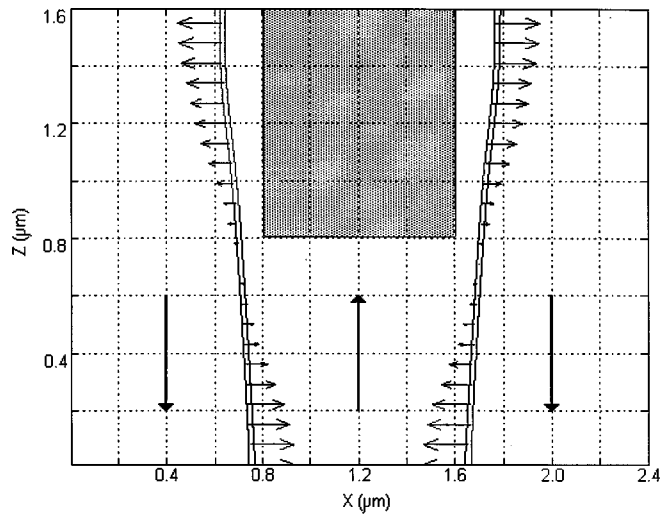


FIG. 2. Cross section of a stripe domain surrounding narrower groove with walls indicated by 33%/66% contours showing magnetization angle ψ . The large arrows indicate the domain magnetization.

The presence of two oppositely magnetized domains perpendicular to the film plane leads to a large stray field. This field has both X and Z components, and is strongest at the surface. The fields from the upper and lower surface are equal and opposite so that the stray field is zero in the center of the sample. The domain walls on each side of the stripe are symmetric with equal and opposite stray fields.

Placing a groove in the surface of the garnet film alters the demagnetizing field in the vicinity. If the groove is within the stripe, the demagnetizing field will be modified such that the equilibrium wall structure shown in Fig. 2 will result.

Adjusting the applied field to reduce the stripe width moves the walls towards the groove. As the wall approaches the groove edge, the stray field of the groove causes ψ to rotate nonuniformly.

Figure 3 shows a wall being driven from a distant point towards the groove. The wall is initially straight, with a uni-

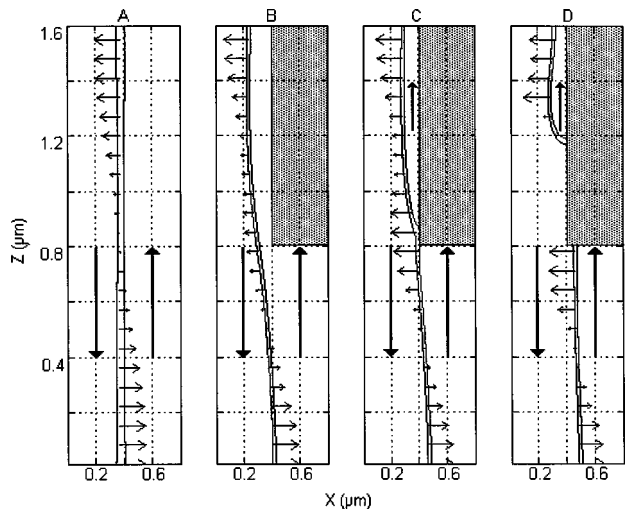


FIG. 3. Deformation of ψ as wall is driven towards groove. (a) Wall far away from groove. (b) Wall close to groove. (c) Wall adjacent to groove. (d) Wall driven underneath groove

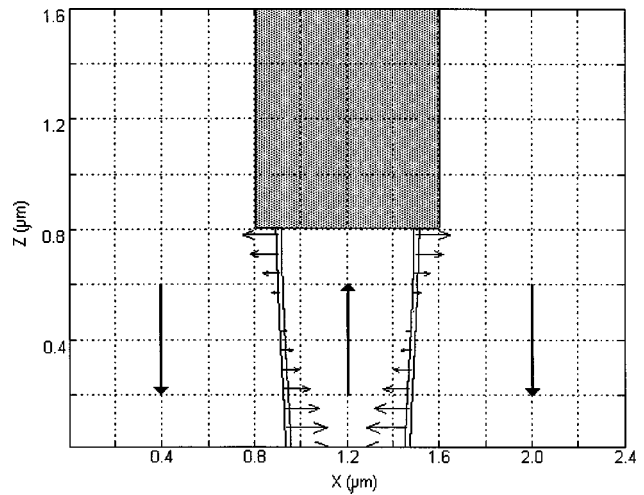


FIG. 4. Cross section of a stripe domain in equilibrium beneath a groove with walls indicated by 33%/66% contours showing the magnetization angle ψ . The large arrows indicate the domain magnetization.

form rotation in ψ [Fig. 3(a)]. As the wall is driven closer to the groove edge, the effect on ψ becomes evident [Figs. 3(b)–3(c)]. At some critical applied field, the break-in field, the wall touches the lower corner of the groove and cleaves, creating a set of disjoint domains [Fig. 3(d)] bounded by a set of head-on walls. The lower wall moves to a stable state beneath the groove. The upper wall, however, is unstable since the domain it bounds is too small to exist. The domain therefore begins to collapse immediately after formation, causing the upper wall to run up the side of the groove. Calculations indicate that the upper wall moves at a velocity on the order of 460 m/s during this process. The break-in field was found to be -200 Oe for the geometry considered here.

Figure 4 shows a stripe in equilibrium underneath a groove: When the bias field is reduced to widen the stripe, the domain expands. As the domain width approaches the

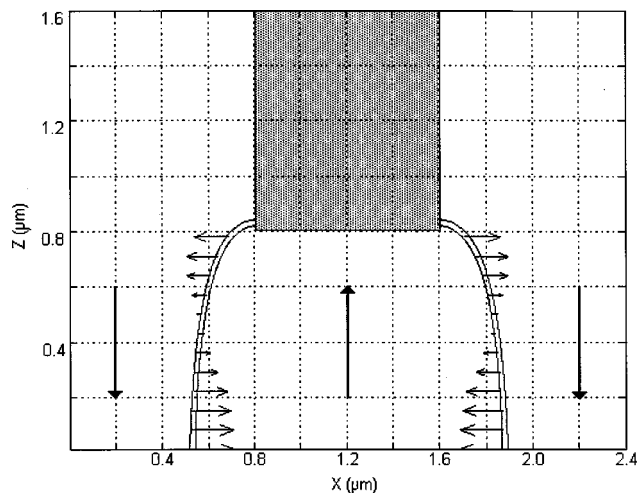


FIG. 5. Cross section of a stripe domain pinned beneath a groove with walls indicated by 33%/66% contours showing the magnetization angle ψ . The large arrows indicate the domain magnetization.

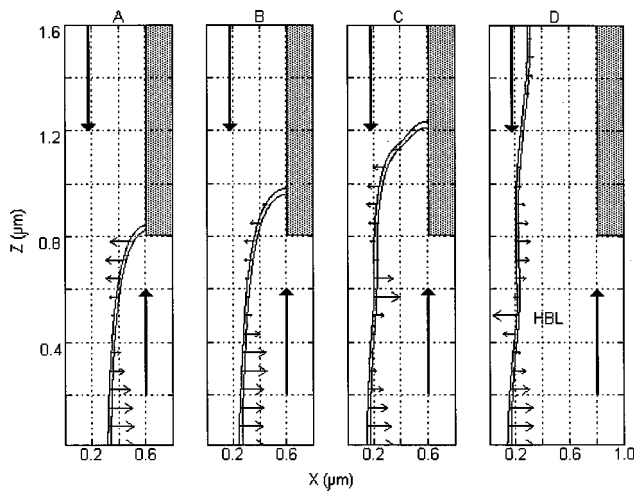


FIG. 6. Domain wall breaking out of groove.

groove width, the groove corners begin to act as pinning sites, as shown in Fig. 5.

Reducing the bias field still further expands the stripe domain beyond the width of the groove. The walls remain pinned by the groove corners, however, leading to the head-on walls depicted in Fig. 5.

Continuing to lower the bias field widens the stripe domain still further. Eventually, the pinning effect of the groove is overcome, and the walls snap away from the groove corners. Figure 6 shows a wall breaking out from a pinned position [Fig. 6(a)] and running up the side of the groove [Fig. 6(b)–6(c)] before moving out of the region [Fig. 6(d)].

The velocity at which the wall climbs the groove during breakout was calculated to be on the order of 300 m/s. This value, as well as that for the velocity during breakin, is dependent upon the applied field. Higher applied fields lead to higher wall velocities. In every case studied, the break-out process has been accompanied by the formation of a horizontal Bloch line (HBL) in the wall, as shown by the region of ψ reversal in Fig. 6.

The width of a wall is usually defined by exchange and anisotropy. For 180° walls, there is seldom any stray field

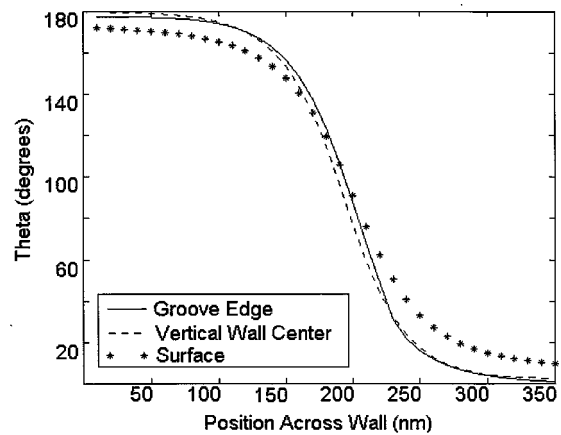


FIG. 7. Magnetization reversal across wall.

present. For a head-on wall, however, there is a large stray field directly across the wall. Despite this, the width of the wall is very similar to that of a “typical” wall. Figure 7 shows this comparison by plotting the polar angle of magnetization, θ , across the wall for the bottom surface, the groove edge (head-on portion), and the center.

It can be seen that the wall widths are essentially the same even though the walls are in greatly different stray fields.

SUMMARY

Grooving has been found to significantly alter the behavior of walls in the immediate vicinity. Wall motion is clearly retarded whenever a groove is approached. This effect occurs both when the wall is pushed out of a groove, and into one. Due to this, it is possible to envision domain confinement being achieved through either a depressed groove or a raised land in the material.

Head-on walls have widths nearly identical to typical walls in the same material despite experiencing a greatly different stray field.

¹S. Gadetsky, T. Suzuki, J. K. Erwin, and M. Manisuripur, *IEEE Trans. Magn.* **30**, 4404 (1994).
²J. C. Wu, R. R. Katti, and H. L. Stadler, *J. Appl. Phys.* **69**, 5751 (1991).
³D. Opalsky and F. B. Humphrey, *IEEE Trans. Magn.* **29**, 2512 (1993).
⁴A. H. Bobeck, *Bell Syst. Tech. J.* **46**, 1901 (1967).